Supporting Information

New nonlinear optical-active $AAgGa_6S_{10}$ (A = K, Rb, Cs) featuring $\{[AgGa_6S_{10}]^-\}_\infty$ framework and high laser damage threshold

Jia-Nuo Li,[a] Xiao-Hui Li,[a] Wen-Dong Yao,[a] Wenlong Liu,[a] and Sheng-Ping Guo*[a]

[a]School of Chemistry and Chemical Engineering, Yangzhou University, Yangzhou, Jiangsu 225002, P. R. China

Experimental Section

Syntheses. The single crystals of $AAgGa_6S_{10}$ (A = K, Rb, Cs) were obtained by a high-temperature solid-state reaction method. For a typical reaction, a 500 mg mixture of starting materials including stoichiometrically weighed Ag_2O (99.7 %), Ga (99.9 %), S (99 %), B (99 %), and additional 250 mg AI (99 %) as the reactive flux was mixed. The mixture was finely powdered in an agate mortar until it has a uniform color (generally gray) and then pressed into a pellet, followed by being loaded into a quartz tube, which had been thoroughly dried. The tube was evacuated to be 1×10^{-4} torr and flame-sealed, which was then put into a muffle furnace, heated from room temperature to 950 ℃ in 24 hours with several intermediate homogenization temperature periods for avoiding binary impurity phases' formation, and kept at 950 ℃ for 7 days, and then cooled to 300 ℃ with a rate of 3 ℃/h, and powered off. The product was washed using distilled water and followed by being ultrasonic washed. Finally, light green transparent single crystals of **1−3** were obtained with probably 80 % yields. The crystals are stable in the air for several months. Because of the different colors and shapes between **1−3** and the impurities, the crystals of **1−3** could be easily separated from the mixture of reaction products under an optical microscope.

Structure Determination. The crystallographic data of **1−3** were collected on a Bruker D8

QUEST X-ray diffractometer equipped with graphite-monochromated Mo-Kα radiation (λ = 0.71073 Å). The structure was solved by Direct Methods and refined by full-matrix least-squares techniques on F^2 with anisotropic displacement parameters for all atoms. All processes were operated by the SHELXTL program package.[1] The final refinements included anisotropic displacements parameters for all atoms and a secondary extinction correction.[2] The crystallographic parameter data are listed in **Table S1**. The atomic coordinates, equivalent isotropic displacement parameters, Wyckoff site, and bond lengths are summarized in **Table S2** and **Table S3**, respectively. Their CIF files have also been deposited with the CCDC number 2056913 for $KAgGa_6S_{10}$, 2056914 for $RbAgGa_6S_{10}$, and 2056915 for $CsAgGa_6S_{10}$.

Powder X-ray Diffraction (PXRD) Characterization. The PXRD patterns of **1−3** were obtained by using a Bruker D8 Advance diffractometer at 40 kV and 100 mA for Cu-Kα radiation (λ = 1.5406 Å) with a scan rate of 5 °/min at room temperature. The simulated patterns were exported using Mercury v3.8 software offered by the Cambridge Crystallographic Data Center and their single-crystal reflection data. The PXRD patterns (**Fig. S1**) corresponds well with the simulated ones, respectively, demonstrating the pure samples for **1−3**.

Infrared (IR) and UV-vis-NIR Diffuse Reflectance Spectra. The IR spectrum was tested by using a Cary 670 FT-IR spectrometer (Agilent Technologies Inc., CA, USA) in the range of 4000–400 cm^{-1}. The diffuse reflectance spectra of **1−3** were collected at room temperature on a computer-controlled Cary 5000 UV–vis–NIR spectrometer equipped with an integrating sphere in the wavelength range of 300–2500 nm. Used a $BaSO_4$ plate as the reference, on which the finely ground powdery sample was covered. The absorption spectra were calculated from the reflection spectra by the Kubelka-Munk function.[3]

Second-Harmonic Generation (SHG) and Powder Laser Damage Threshold (LIDT) Measurements. SHG measurement was executed by a modified Kurtz-Perry NLO method with a 2.1 μm Q-switch laser radiation as the light source.[4] For the size-dependent SHG measurement, polycrystalline powdery samples of **1−3** were sieved into different particle size ranges of 25~45, 45~75, 75~110, 110~150, 150~210, and 210~250 μm, respectively. And so do the same thing to benchmark $AgGaS_2$ (AGS) samples as standard. Each sample was loaded into a customized box that could transmit light. After that, a pulsed IR beam from a Q-switched

2.1 μm laser traverse the prepared boxes. The SHG signals were collected by a photomultiplier tube and the peaks appeared on the oscilloscope.

The single-pulse measurement method was used to measure the LIDT values of **1−3**. The crystalline samples of **1−3** and AGS with the same size range of 75~110 μm were loaded into glass microscope cover slides and a 1064 nm laser with a pulse width τ_p of 10 ns in a 1 Hz repetition irradiate on it. The tests were carried out under an optical microscope once single-pulse radiation passed, and the laser power increased until the damaged spot was observed. Then, the laser power was marked, and the area of the damaged spot was measured as the damage threshold parameters of the sample. The laser beam power is monitored by the Nova II sensor display and the PE50-DIT-C energy sensor. The damaged point is measured with a vernier caliper.

Calculation Details. The single-crystal diffraction data of **1−3** provide the calculation models. The CASTEP module in Material Studio software is used to calculate the band structure, density of states (DOS) and optical properties.[5] The exchange-correlation function GGA (generalized gradient approximation) was chosen and a plane wave which basis on the Perdew-Burke-Enzerhof (PBE)-type exchange-correlation potentials was used. The plane-wave cutoff energy was 330 eV, and set the threshold of 5×10^{-7} eV/atom for the self-consistent-field convergence of the total electronic energy. The electronic configurations for K, Rb, Cs, Ag, Ga, and S were $4s^1$, $5s^1$, $6s^1$, $4d^{10}5s^1$, $4s^24p^1$, and $3s^23p^4$, respectively. The numerical integration of the Brillouin zones was performed using $2 \times 2 \times 3$ Monkhorst–Pack k-point meshes and choose the Fermi level at 0 eV as the reference.

The optical properties were calculated and described by the complex dielectric function $\varepsilon(\omega)$ = $\varepsilon_1(\omega) + i\varepsilon_2(\omega)$. $\varepsilon_1(\omega)$ represents the real part and $i\varepsilon_2(\omega)$ represents the imaginary part of the dielectric function.[6,7] $\varepsilon_2(\omega)$ can be used to generate other optical constants using the Kramers-Kroning transform.[8,9] The first-order non-resonant susceptibility in the low frequency region is $x^{(1)}(\omega) = \varepsilon_1(\omega) - 1$, and the second order susceptibility can be expressed as the first order susceptibility.[10,11]

Table S1. Crystal data and structure refinement parameters for **1−3**.

Chemical formula	$KAgGa_6S_{10}$ (1)	$RbAgGa_6S_{10}$ (2)	$CsAgGa_6S_{10}$ (3)
Fw	885.89	932.26	979.70
T (K)	296(2)	296(2)	296(2)
crystal system	monoclinic	monoclinic	monoclinic
space group	Cc	Cc	Cc
Z	4	4	4
unit cell parameters (Å)	$a = 16.8278(11)$	$a = 16.823(2)$	$a = 16.8381(6)$
	$b = 6.4318(4)$	$b = 6.4449(9)$	$b = 6.4655(3)$
	$c = 16.1146(10)$	$c = 16.163(2)$	$c = 16.2525(6)$
$V(Å^3)$	1625.07(18)	1632.7(4)	1648.71(11)
D_{calc} (g cm^{-3})	3.621	3.793	3.947
μ (mm^{-1})	12.487	35.973	14.232
$F(000)$	1648.0	1720.0	1792.0
2θ range (º)	5.196 to 50.958	7.316 to 50.998	5.192 to 50.996
indep. reflns/R_{int}	2949/ 0.0269	2663/ 0.0386	2976/ 0.0368
GOF on F^2	0.836	0.955	0.831
$R1$, wR2 ($I > 2\sigma(I)$)[a]	0.0117, 0.0283	0.0207, 0.0412	0.0157, 0.0372
R1, wR2 (all data)[a]	0.0119, 0.0284	0.0216, 0.0416	0.0160, 0.0374

[a]$R1 = ||F_o| - |F_c||/|F_o|$; [b]$wR2 = [w(F_o^2 - F_c^2)^2]/[w(F_o^2)^2]^{1/2}$.

Table S2. Atomic coordinates ($\times 10^4$) and equivalent isotropic displacement parameters ($U_{eq}{}^a$, $\text{Å}^2 \times 10^3$) for **1−3**.

Atom	Wyck. site	x	y	z	$U_{eq}/\text{Å}^2$
			1		
K	4a	3070.9(9)	6935.3(2)	3530.9(9)	47.7(3)
Ag	4a	5790.0(2)	1748.4(4)	1804.8(3)	22.75(1)
Ga(1)	4a	522.1(3)	1596.4(5)	2826.5(3)	9.66(1)
Ga(2)	4a	1362.1(4)	1643.4(5)	1052.0(4)	9.84(1)
Ga(3)	4a	1874.5(3)	3204.9(6)	5104.3(3)	9.72(1)
Ga(4)	4a	3646.4(3)	3130.3(5)	1506.6(3)	9.99(1)
Ga(5)	4a	4021.8(3)	1737.1(6)	5529.2(3)	9.61(1)
Ga(6)	4a	5032.6(3)	1781.9(6)	3702.0(4)	9.54(1)
S(1)	4a	0.0(6)	1651.5(1)	0.0(6)	9.7(2)
S(2)	4a	464.8(6)	3345.2(1)	4071.7(6)	8.5(2)
S(3)	4a	1437.7(7)	3194.2(1)	2323.9(7)	11.4(2)
S(4)	4a	1938.2(7)	1559.2(1)	6356.8(7)	11.5(2)
S(5)	4a	2249.5(6)	3354.9(1)	484.2(6)	9.9(2)
S(6)	4a	2771.9(6)	2297.8(1)	4433.1(6)	14.85(2)
S(7)	4a	3669.2(7)	1813.1(1)	2793.7(7)	15.4(2)
S(8)	4a	4117.6(6)	6590.2(1)	1836.9(7)	9.8(2)
S(9)	4a	4326.4(7)	1706.1(1)	667.4(7)	12.2(2)
S(10)	4a	6028.5(7)	3421.0(1)	3325.3(6)	11.5(2)
			2		
Rb	4a	3110.3(5)	6936.3(1)	3531.3(6)	30.12(2)
Ag	4a	5812.7(4)	1742.7(7)	1830.9(4)	21.61(2)
Ga(1)	4a	526.0(5)	1598.7(9)	2823.7(5)	9.11(2)
Ga(2)	4a	1362.4(7)	1660.6(9)	1045.0(7)	9.31(2)
Ga(3)	4a	1875.8(5)	3189.8(10)	5101.1(5)	9.1(2)
Ga(4)	4a	3653.3(6)	3142.5(9)	1509.8(6)	9.5(2)
Ga(5)	4a	4026.3(5)	1715.1(10)	5536.2(5)	9.4(2)

Ga(6)	4a	5033.7(5)	1786.5(1)	3699.3(6)	9.3(2)
S(1)	4a	0.0(1)	1680(2)	0.0(1)	8.9(3)
S(2)	4a	469.9(1)	3356.2(2)	4063.3(1)	8.1(3)
S(3)	4a	1446.8(1)	3176(2)	2323.0(1)	10.7(4)
S(4)	4a	1930.4(1)	1542(2)	6344.8(1)	11.0(4)
S(5)	4a	2256.3(1)	3382(2)	486.7(1)	9.0(4)
S(6)	4a	2774.0(1)	2232(2)	4443.1(1)	13.3(3)
S(7)	4a	3671.4(1)	1829(2)	2789.8(1)	14.1(4)
S(8)	4a	4125.3(1)	6594(2)	1834.3(1)	9.0(4)
S(9)	4a	4348.4(1)	1707(2)	694.7(1)	11.4(4)
S(10)	4a	6030.3(1)	3435(2)	3333.4(1)	10.7(4)
3					
Cs	4a	3138.3(3)	6931.2(5)	3544.3(2)	20.42(1)
Ag	4a	5837.2(3)	1729.4(6)	1865.2(4)	21.14(2)
Ga(1)	4a	527.7(5)	1600.9(8)	2820.3(5)	9.20(2)
Ga(2)	4a	1359.7(6)	1678.4(8)	1039.1(6)	9.12(2)
Ga(3)	4a	1875.5(4)	3175.4(9)	5102.4(5)	9.06(2)
Ga(4)	4a	3659.6(5)	3153.3(8)	1517.2(6)	9.32(2)
Ga(5)	4a	4031.1(5)	1692.1(9)	5546.7(4)	9.17(2)
Ga(6)	4a	5031.8(5)	1788.0(9)	3697.2(5)	9.10(2)
S(1)	4a	-0.1(1)	1729(2)	0.2(1)	9.4(3)
S(2)	4a	480.3(1)	3375.9(2)	4051.4(1)	8.4(3)
S(3)	4a	1450.8(1)	3146.8(2)	2319.2(1)	11.0(3)
S(4)	4a	1908.8(1)	1524(2)	6326.1(1)	11.3(3)
S(5)	4a	2261.6(9)	3411.1(2)	497.7(1)	9.2(3)
S(6)	4a	2774.1(1)	2144(2)	4464.1(1)	12.6(3)
S(7)	4a	3674.3(1)	1839.8(2)	2785.8()	13.0(3)
S(8)	4a	4130.7(1)	6590(2)	1828.5(1)	9.6(3)
S(9)	4a	4374.2(1)	1701.5(2)	736.9(1)	10.7(3)

S(10)	4a	6026.0(9)	3457.8(2)	3342.5(1)	11.0(3)

$^{a}U_{eq}$ is defined as one third of the trace of the orthogonalized U_{ij} tensor.

Table S3. Important bond lengths (Å) for **1−3**.

Bond	Distance/Å	Bond	Distance/Å
1			
K−S(3)	3.639(2)	Ga(2)−S(4)#8	2.253(9)
K−S(4)#2	3.463(2)	Ga(2)−S(5)	2.296(1)
K−S(6)	3.434(2)	Ga(3)−S(2)	2.353(1)
K−S(7)	3.761(1)	Ga(3)−S(4)	2.247(1)
K−S(7)#3	3.624(1)	Ga(3)−S(5)#4	2.321(1)
K−S(8)	3.755(2)	Ga(3)−S(6)	2.231(1)
K−S(9)#4	3.435(2)	Ga(4)−S(5)	2.334(1)
K−S(10)#1	3.465(2)	Ga(4)−S(7)	2.228(1)
Ag−S(3)#5	2.540(9)	Ga(4)−S(8)	2.358(9)
Ag−S(4)#6	2.540 (1)	Ga(4)−S(9)	2.259(1)
Ag−S(9)	2.479(1)	Ga(5)−S(1)#9	2.352(1)
Ag−S(10)	2.571(1)	Ga(5)−S(6)	2.231(1)
Ga(1)−S(2)	2.333(1)	Ga(5)−S(8)#4	2.319(1)
Ga(1)−S(3)	2.235(1)	Ga(5)−S(9)#10	2.266(9)
Ga(1)−S(8)#7	2.322(1)	Ga(6)−S(1)#9	2.340(1)
Ga(1)−S(10)#7	2.246(9)	Ga(6)−S(2)#5	2.336(9)
Ga(2)−S(1)	2.304(1)	Ga(6)−S(7)	2.229(1)
Ga(2)−S(3)	2.241(1)	Ga(6)−S(10)#2	2.242(1)
2			
Rb−S(2)#2	3.854(2)	Ga(2)−S(3)	2.242(2)
Rb−S(3)	3.681(2)	Ga(2)−S(4)#9	2.252(2)
Rb−S(4)#3	3.506(2)	Ga(2)−S(5)	2.301(2)
Rb−S(5)#4	3.924(2)	Ga(3)−S(2)	2.353(2)

Rb−S(6)#5	3.840(2)	Ga(3)−S(4)	2.246(2)
Rb−S(6)	3.506(2)	Ga(3)−S(5)#4	2.322(2)
Rb−S(7)#5	3.619(2)	Ga(3)−S(6)	2.228(2)
Rb−S(7)	3.739(2)	Ga(4)−S(5)	2.336(2)
Rb−S(8)	3.727(2)	Ga(4)−S(7)#4	2.225(2)
Rb−S(9)#4	3.470(2)	Ga(4)−S(8)	2.356(2)
Rb−S(10)#1	3.531(2)	Ga(4)−S(9)	2.254(2)
Ag−S(3)#6	2.537(2)	Ga(5)−S(1)#10	2.353(2)
Ag−S(4)	2.539(19)	Ga(5)−S(6)	2.228(2)
Ag−S(9)#4	2.481(2)	Ga(5)−S(8)#4	2.316(2)
Ag−S(10)#6	2.564(2)	Ga(5)−S(9)#11	2.263(2)
Ga(1)−S(2)	2.333(2)	Ga(6)−S(1)#10	2.342(2)
Ga(1)−S(3)	2.236(2)	Ga(6)−S(2)#6	2.336(2)
Ga(1)−S(8)#8	2.318(2)	Ga(6)−S(7)	2.228(2)
Ga(1)−S(10)#8	2.247(2)	Ga(6)−S(10)	2.239(2)
Ga(2)−S(1)	2.301(2)		
3			
Cs−S(1)#1	3.955(2)	Ga(2)−S(3)	2.241(2)
Cs−S(2)#3	3.840(2)	Ga(2)−S(4)#10	2.246(1)
Cs−S(3)	3.731(2)	Ga(2)−S(5)	2.303(2)
Cs−S(4)#4	3.587(2)	Ga(3)−S(2)	2.354(2)
Cs−S(6)	3.586(2)	Ga(3)−S(5)#6	2.240(2)
Cs−S(6)#5	3.826(1)	Ga(3)−S(6)	2.324(1)
Cs−S(7)#5	3.635(1)	Ga(3)−S(5)	2.225(2)
Cs−S(7)	3.739(1)	Ga(4)−S(7)	2.342(2)
Cs−S(8)	3.742(2)	Ga(4)−S(8)	2.222(2)
Cs−S(9)#6	3.525(2)	Ga(4)−S(9)	2.352(2)
Cs−S(10)#1	3.590(2)	Ga(4)−S(8)#2	2.246(2)
Ag−S(3)#7	2.535(1)	Ga(5)−S(1)#2	2.355(2)

Ag—S(4)#8	2.539(2)	Ga(5)—S(6)	2.227(2)
Ag—S(9)	2.480(2)	Ga(5)—S(8)#6	2.313(2)
Ag—S(10)	2.561(2)	Ga(5)—S(9)#12	2.261(2)
Ga(1)—S(2)	2.333(2)	Ga(6)—S(1)#2	2.343(2)
Ga(1)—S(3)	2.235(2)	Ga(6)—S(2)#7	2.343(2)
Ga(1)—S(8)#9	2.319(2)	Ga(6)—S(7)	2.335(1)
Ga(1)—S(10)#9	2.244(1)	Ga(6)—S(10)	2.228(2)
Ga(2)—S(1)	2.300(2)		

Symmetry transformation used to generate equivalent atoms: Compound **1**: +x, +y, 1+z; +x, 1-y, 1/2+z; +x, 2-y, 1/2+z; +x, -1+y, 1+z; 1/2+x, 3/2-y, 1/2+z; +x, -1+y, +z; 1/2+x, 3/2-y, -1/2+z; +x, 1+y, +z; 1/2+x, 1/2+y, +z; +x, 2-y, -1/2+z; -1/2+x, 1/2+y, +z; +x, 1-y, -1/2+z; +x, 1+y, -1+z; -1/2+x, -1/2+y, +z; -1/2+x, 3/2-y, 1/2+z; 1/2+x, -1/2+y, +z; +x, +y, -1+z; -1/2+x, 3/2-y, -1/2+z. Compound **2**: +x, 1-y, -1/2+z; -1/2+x, 1/2-y, -1/2+z; +x, -y, -1/2+z; +x, 1+y, +z; -1/2+x, 1/2+y, +z; 1/2+x, 1/2-y, 1/2+z; +x, -1+y,+z; -1/2+x, -1/2-y, -1/2+z; -1/2+x, -1/2+y, +z; 1/2+x, -1/2+y, +z; 1/2+x, 1/2+y, +z; +x, 1-y, 1/2+z; +x, -y, 1/2+z; 1/2+x, -1/2-y, 1/2+z. Compound **3**: -1/2+x, -3/2-y, 1/2+z; -1/2+x, -1/2+y, +z; +x, -2-y, 1/2+z; +x, -1+y, +z; -1/2+x, -5/2-y, 1/2+z; +x, -2-y, -1/2+z; +x, -1-y, -1/2+z; +x, 1+y, +z; 1/2+x, 1/2+y, +z; +x, -1-y, 1/2+z; 1/2+x, -1/2+y, +z; 1/2+x, -3/2-y, -1/2+z; -1/2+x, 1/2+y, +z; 1/2+x, -5/2-y, -1/2+z.
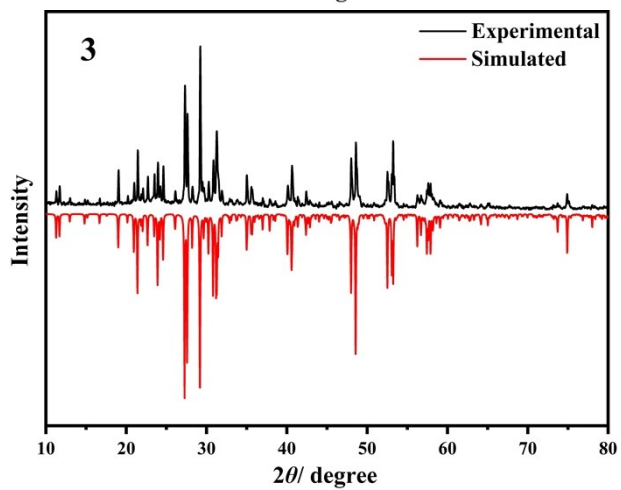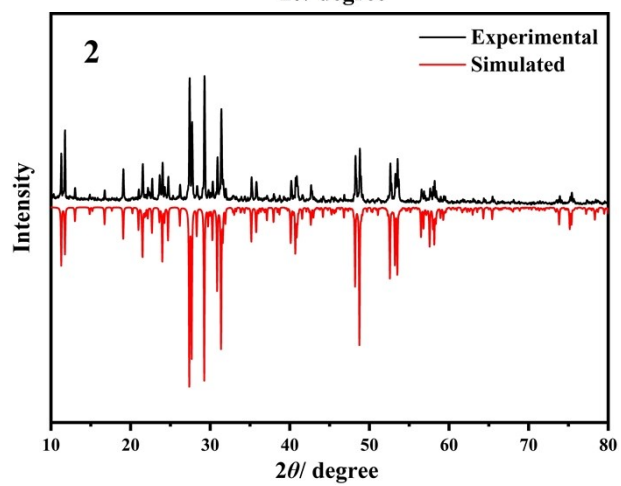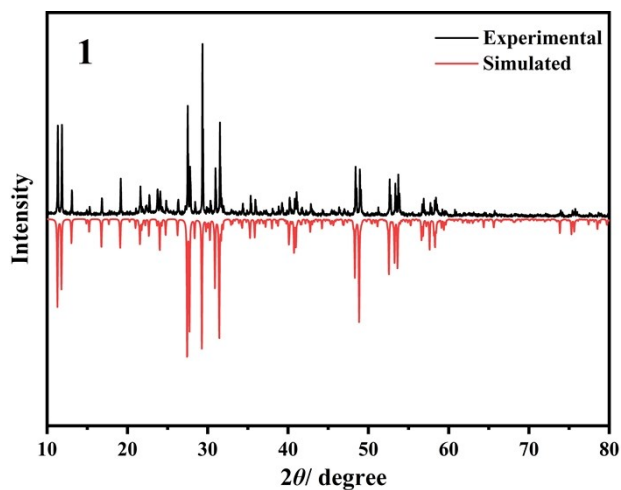
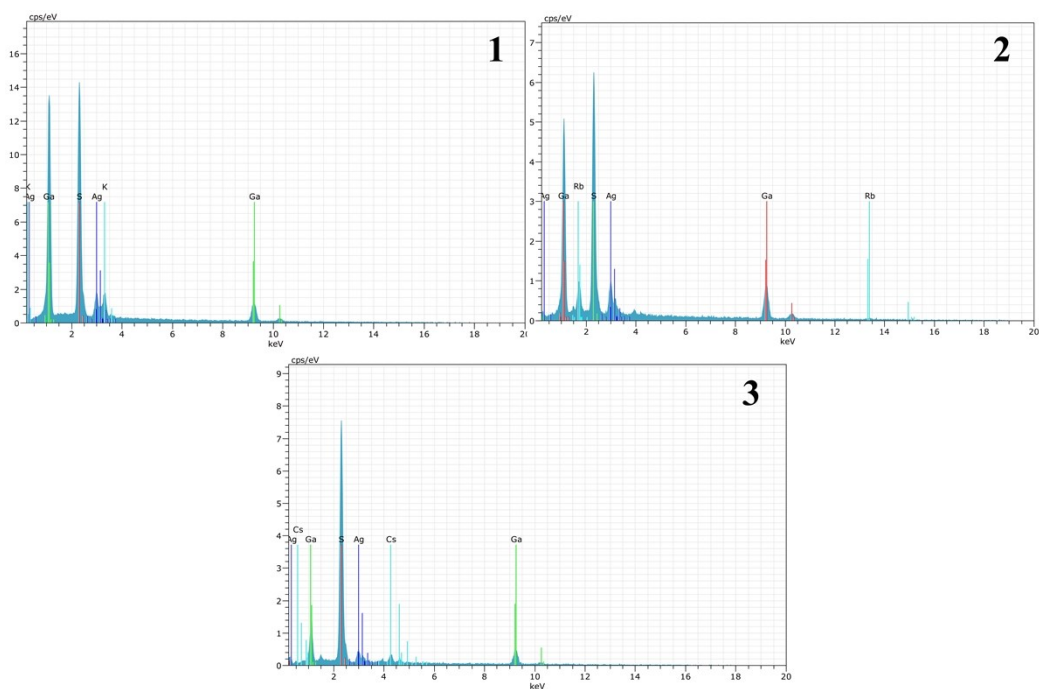**Fig. S1** Powder X-ray diffraction patterns for **1**−**3**.

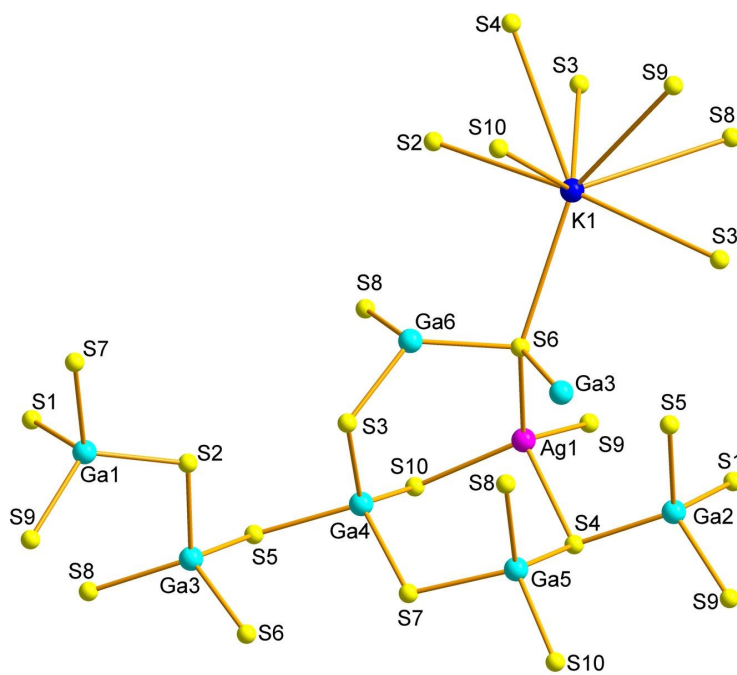**Fig. S2** Energy dispersive spectroscopes for single crystals of **1−3**.

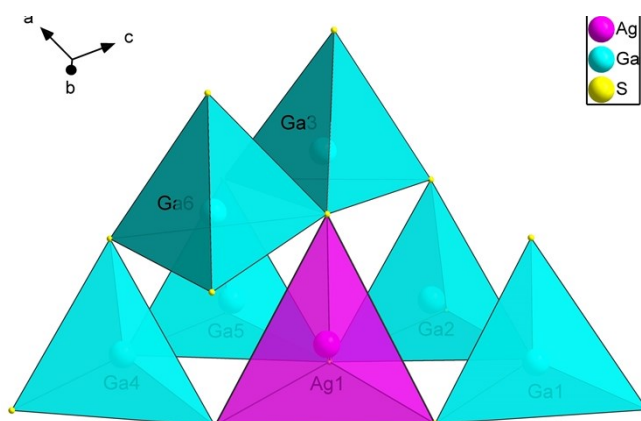**Fig. S3** Coordination geometry of **1**.

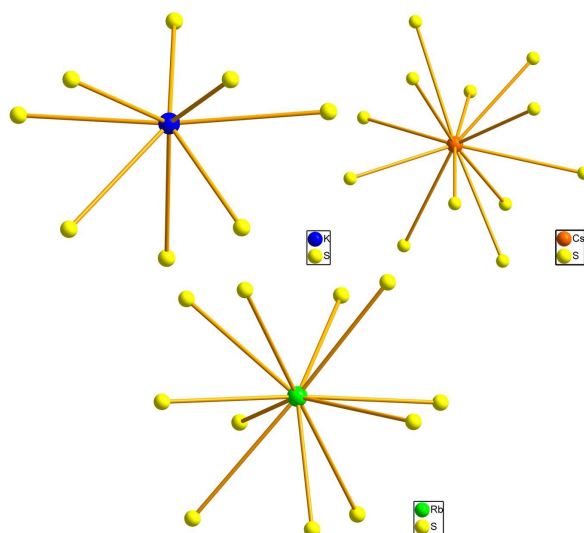**Fig. S4** Each AgS$_4$ tetrahedron share corners with six neighboring GaS$_4$ tetrahedra in **1–3**.

Fig. S5 Coordination configurations for alkali metal cations in **1−3**.
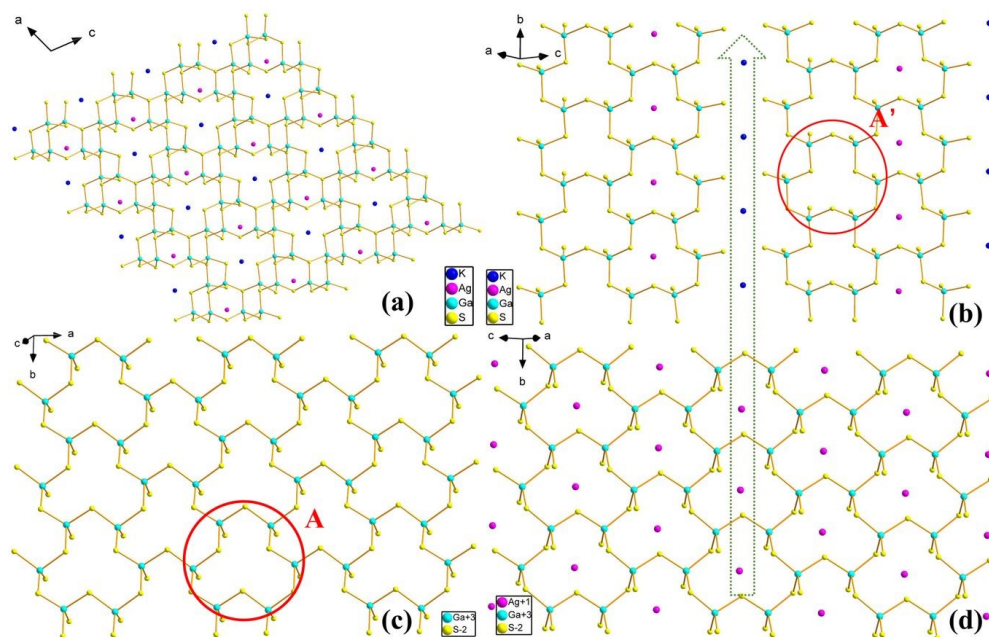
Fig. S6 The structure relationship between **1**, AGS, and *m*-Ga$_2$S$_3$ when considered from the basic structural layer that build the structures.
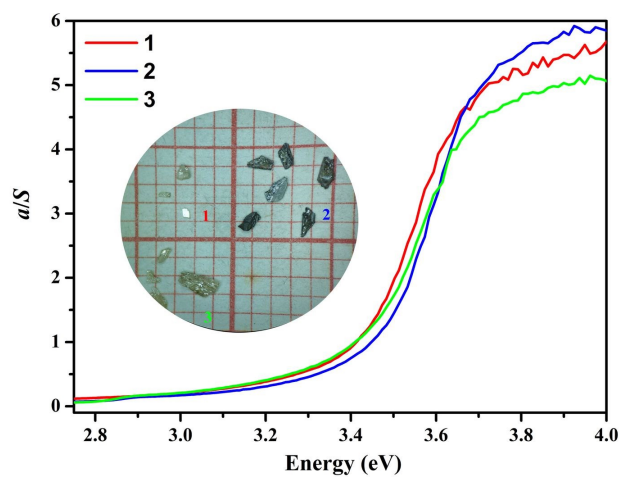
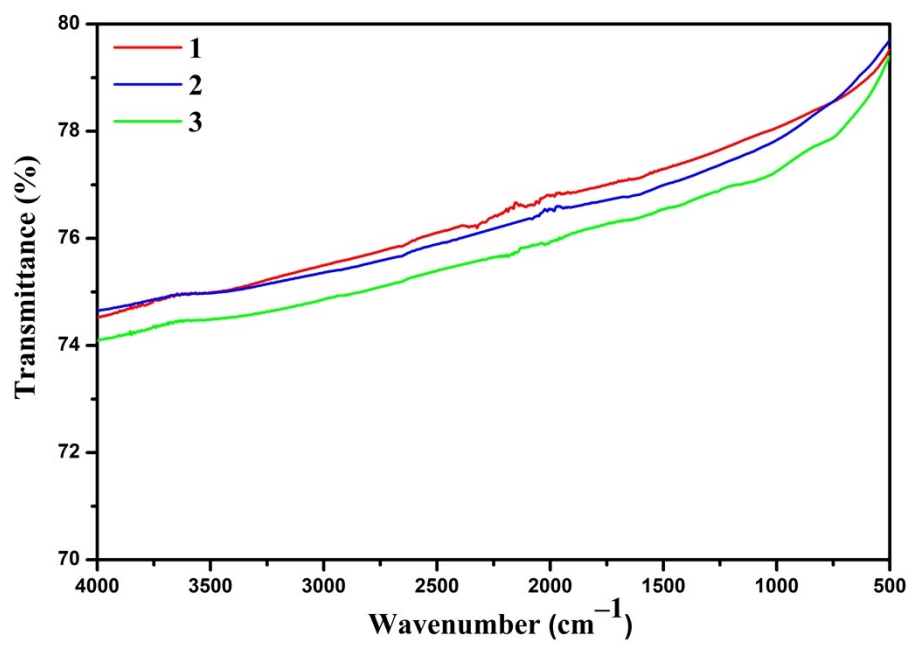**Fig. S7** UV-*vis*-NIR diffuse reflectance spectra and single crystal photos of **1−3**.

Fig. S8 Fourier transform infrared spectra of **1−3** measured from 400 to 4000 cm^{-1}.
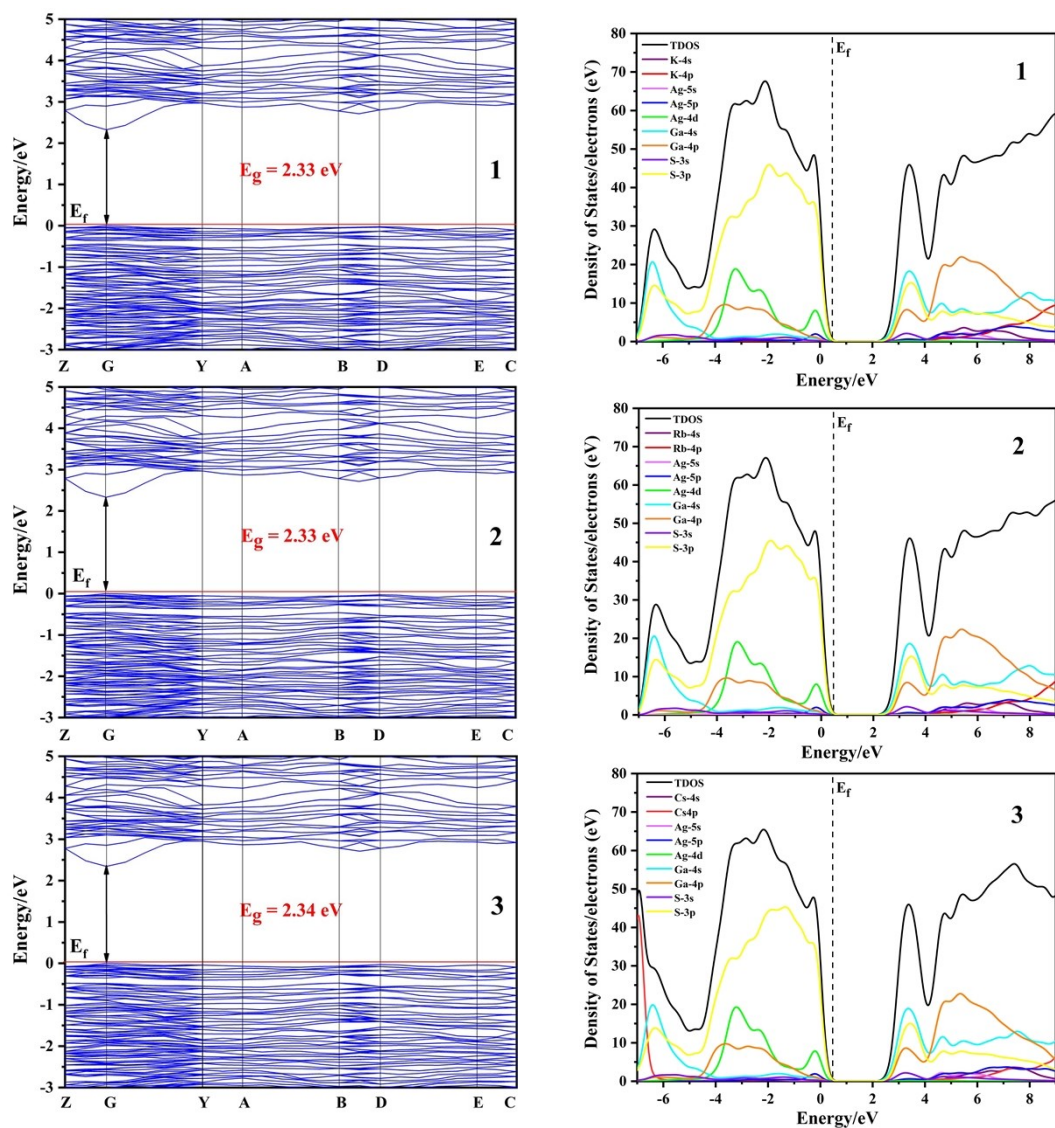
Fig. S9 Calculated band structures (left) and density of states (DOS, right) for **1−3**. Fermi level is chosen at 0 eV.
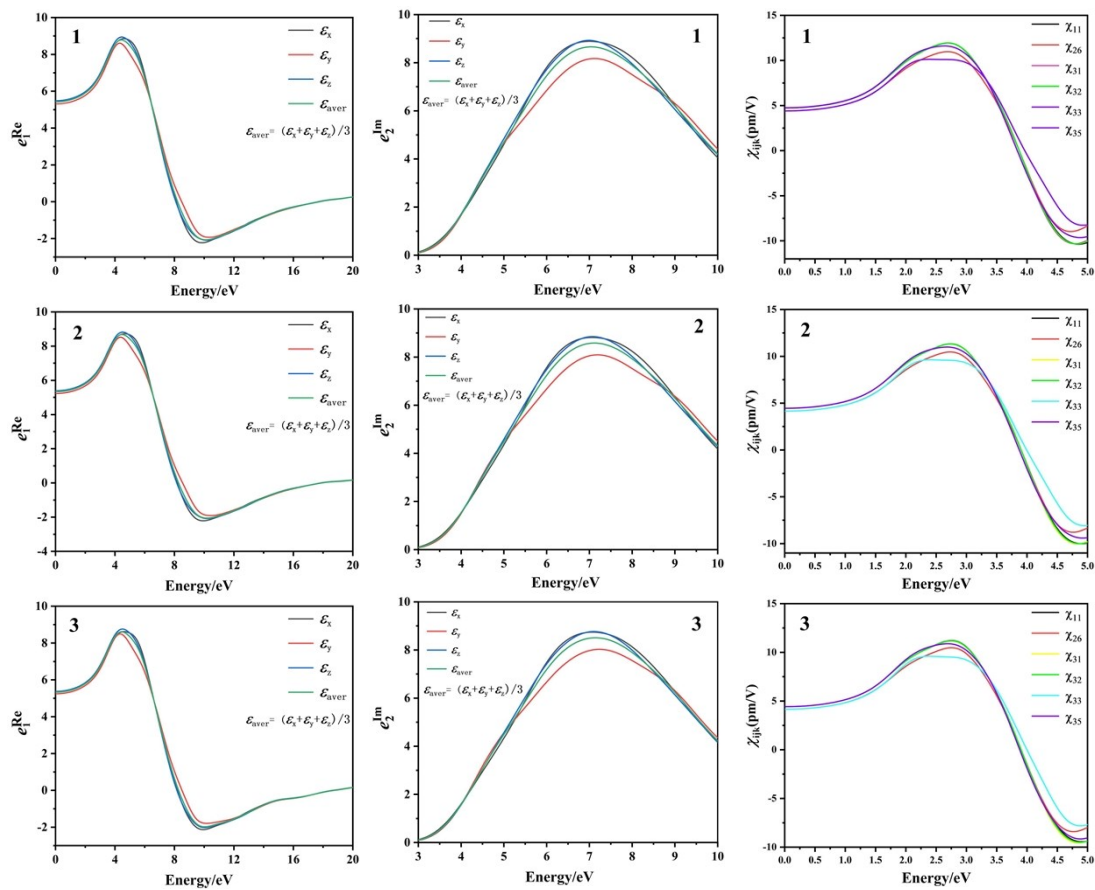
Fig. S10 Calculated real (left) and imaginary (middle) parts of optical dielectric constants and frequency-dependent SHG tensors (right) for **1−3**.

References

1   O. V. Dolomanov, L. J. Bourhis, R. J. Gildea, J. A. K. Howard and H. Puschmann, *J. Appl. Crystallogr.*, 2009, **42**, 339.

2   G. M. Sheldrick, *Acta Crystallogr. C*, 2015, **71**, 3−8.

3   (a) W. W. Wendlandt and H. G. Hecht, *Reflectance Spectroscopy*, Interscience Publishers, New York, **1966**; (b) G. Kortüm, *Reflectance Spectroscopy*, Springer, 1969.

4   S. K. Kurtz and T. T. Perry, *J. Appl. Phys.*, 1968, **39**, 3798−3813.

5   S. J. Clark, M. D. Segall, C. J. Pickard, P. J. Hasnip, M. I. Probert, K. Refson and M. C. Payne, *Z. Kristallogr.-Cryst. Mater.*, 2005, **220**, 567−570.

6   F. Bassani and G. P. Parravicini, *Electronic States and Optical Transitions in Solid*s; Pergamon Press Ltd.: Oxford, U.K., 1976.

7   M. Gajdoš, K. Hummer, G. Kresse, J. Furthmüller and F. Bechstedt, *Phys. Rev. B*, 2006, **73**, 045112.

8   S. Laksari, A. Chahed, N. Abbouni, O. Benhelal and B. Abbar, *Comp. Mater. Sci.*, 2006, **38**, 223−230.

9   S. D. Mo and W. Y. Ching, *Phys. Rev. B*, 1995, **51**, 13023.

10   C. S. Aversa and J. E. Sipe, *Phys. Rev. B*, 1995, **52**, 14636.

11   S. N. L. Rashkeev, W. R. L. Lambrecht and B. Segall, *Phys. Rev. B*, 1998, **57**, 3905.